RSC Advances

ROYAL SOCIETY
OF CHEMISTRY

www.rsc.org/advances

Synthesis and Property of a Novel Cu(II)−pyridineoxazoline Containing Polymeric Catalyst for Asymmetric Diels−Alder Reaction

Soluble and recyclable Cu(II)−pyridineoxazoline containing polymeric catalyst shows faster reaction rate and higher enantio-selectivity than its low molecular mass counterpart in catalyzing Diels−Alder reaction of 2-alkenyol pyridine *N*-oxide and cyclopentadiene.

Ar = 4-nitrophenyl, ee = 52%
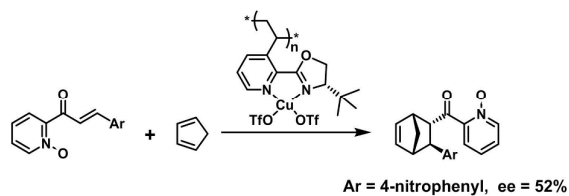
ARTICLE TYPE

Synthesis and Property of a Novel Cu(II)−pyridineoxazoline Containing Polymeric Catalyst for Asymmetric Diels−Alder Reaction

Heng Wang, Na Li, Zijia Yan, Jie Zhang and Xinhua Wan[*]

A novel pyridineoxazoline (PyOx) containing optically active polymer, poly[(−)-(*S*)-4-*tert*-butyl-2-(3-vinylpyridin-2-yl)-oxazoline], was prepared via the radical polymerization of (−)-(*S*)-4-*tert*-butyl-2-(3-vinylpyridin-2-yl)-oxazoline. Its complex with Cu(OTf)$_2$ was employed to catalyze homogeneous Diels−Alder (D−A) reaction of 2-alkenyol pyridine *N*-oxide and cyclopentadiene in tetrahydrofuran. The
10 polymeric catalyst showed a 5 fold faster reaction rate and a 2.5 fold higher enantio-selectivity than the Cu(II) complex of (−)-(*S*)-4-*tert*-butyl-2-(3-methylpyridin-2-yl)-oxazoline, a low molecular mass model compound. This was rationalized by the constrained environment around catalytic site provided by the polymer backbone in terms of CD spectrometry results. The polymer complex was easily recycled by the precipitation method, and only a slight decrease of reactivity and enantio-selectivity was observed after 5
15 cycles.

Introduction

Asymmetric catalysis, which produces enantiomerically rich or pure compounds, has received increased attention in the past decade and is playing dominant roles in contemporary organic
20 chemistry.[1-3] Although a great number of organometallic catalysts and organocatalysts have been developed, few of them are applied in mass production because of the unacceptable cost performance ratio as well as the complexity of catalyst preparation.[4, 5] Immobilization of the catalysts to polymer matrix
25 is one of the helpful methods to solve the problems owing to the ease of recycling by filtration or centrifugation.[6]

Generally, two strategies have been developed to introduce catalytically functional groups to polymers. One is tethering the catalytic groups to the polymer matrix via flexible spacers with a
30 relatively low density, in order to diminish the influence from the polymer backbone and maintain the efficiency and enantio-selectivity of the catalytic sites.[7-10] Another one is attaching the functional groups to polymer backbone directly or via rigid spacers, or utilizing them as building blocks of a polymer chain.
35 The latter takes the advantage of the cooperation between the polymer matrix and catalytic species to enhance the reactivity and enantio-selectivity of chemical reaction. Helical polymers outstand other macromolecular scaffolds by providing additional asymmetric environment as enzymes.[11] Asymmetric allylic
40 substitution of 1,3-diphenylprop-2-enyl acetate and allylation of benzaldehyde catalyzed by pyridine derived poly(trityl methacrylate),[12, 13] Henry reaction of aldehydes with nitromethane by cinchona alkaloid tethered poly(phenylacetylene),[14] addition reaction of aldehydes with
45 diethylzinc by chiral polybinaphthols,[15] as well as hydrosilylation of styrene by phosphine-palladium complex bonded

polyquinoxaline[16] have fully revealed the potentials of such polymeric catalysts in asymmetric synthesis. Interestingly, the configuration of hydrosilylation product could be switched by
50 reversing the screw sense of helical polyquinoxaline by changing solvent without loss of ee%.

Bis(oxazoline) (BOX) derivatives are among the most successful ligands of organometallic catalysts in catalyzing a great number of asymmetric reactions with an excellent yield and
55 enantio-selectivity.[17, 18] The effects of the linker between two oxazoline rings, achiral bulky groups and chiral groups on oxazoline rings as well as central metals have been well investigated.[17, 19-24] The immobilization of BOX to polymer matrix has been fully developed to recycle the catalyst.[24-27]
60 Mono(oxazoline) inherits most advantages of BOX, but is easier to prepare and consumes less amount of chiral agents than BOX.[28-30] Pyridineoxazoline (PyOx) metal complex has excellent enantio-selectivity in catalyzing allylic alkylation reaction,[31, 32] Heck-type reactions[33-36] and Wacker-type cyclizations.[9, 40]
65 However, it is very seldom to catalyze asymmetric Diels−Alder (D−A) reaction, which was the most powerful way to prepare six membered carbocycles or heterocycles with four stereogenic centers in a stereocontrolled manner,[41] probably owing to its lack of C$_2$ symmetric axis as well as its less bulky geometry. A few
70 PyOx−Cu(II) complex containing polymers have been reported,[40-43] but have never been applied in asymmetric D−A reaction. Martinez-Merino *et al* introduced the PyOx group onto the backbone of cross-linked polystyrene.[42, 43] Its Cu(II) complex was applied in asymmetric cyclopropanation of styrene with an
75 enhancement in enantio-selectivity compared with the small molecular complex.

The present work aimed to develop a soluble and recyclable chiral polymeric organometallic catalyst of asymmetric D−A

reaction, based on the coordination of Cu(OTf)$_2$ and poly[(−)-(*S*)-4-*tert*-butyl-2-(3-vinylpyridin-2-yl)-oxazoline] (**P1**). The direct connection of the catalytic sites to the polymer main chain was expected to enhance their interactions and improve the enantio-
5 selectivity of chemical transformation. Such a macromolecular architecture might also favour the formation of helical conformation of polymer chains. Compared to a low molecular mass model compound, the polymeric catalyst showed five fold faster reaction rate, and two and a half fold higher enantio-
10 selectivity in the D−A reaction of 2-akenyol pyridine *N*-oxide and cyclopentadiene in tetrahydrofuran, although no chiral secondary structure was generated. Owing to the good solubility of polymeric catalyst in THF, circular dichroism (CD) spectrometry was utilized to understand the influence of the backbone to the
15 enantio-selectivity.

Experimental Section

Solvents and Reagents

3-Methylpicolinonitrile (98%, J&K Scientific Ltd.), tetrachloromethane (CCl$_4$, AR, Beijing Chemical Co.), *N*-
20 bromosuccinimide (NBS, 99%, Aldrich), triphenylphosphine (PPh$_3$, 99%, Acros), aqueous formaldehyde (40%, AR, Beijing Chemical Co.), (*S*)-*tert*-leucinol (97%, TCI Co. Ltd.), zinc(II) triflate (Zn(OTf)$_2$, 98%, J&K Scientific Ltd.) and copper(II) triflate (Cu(OTf)$_2$, 98%, J&K Scientific Ltd.) were used as
25 purchased. Azobisisobutyronitrile (AIBN, AR, Wuhan Chemical Co.) was recrystallized from ethanol three times and dried under vacuum at room temperature. Tetrahydrofuran (THF, AR, Beijing Chemical Co.) was refluxed over sodium and distilled out just before use. Cyclopentadiene was freshly cracked and distilled
30 from its dimer. The substrates, 2-alkenoyl pyridine *N*-oxides (**4a~d**), were prepared followed the literature method and the detailed procedures were described in the supplementary information.[44]

Measurements

35 ^{1}H-NMR (400 MHz) and ^{13}C-NMR (100 MHz) spectra were recorded on a Bruker ARX400 spectrometer at room temperature in CDCl$_3$ with tetramethylsilane (TMS) as an internal standard. Mass spectra were collected on a Bruker Apex IV FTMS mass spectrometer. Elemetary analyses were carried out on an
40 Elementar Vario MICRO CUBE instrument. The weight- and number-average molecular weights (M_w and M_n, respectively) were estimated by a gel permeation chromatography (GPC) apparatus equipped with a Waters 2410 refractive-index detector and a Waters 515 pump. Three Waters Styragel columns with a
45 10 μm bead size were connected in series. Their effective molecular weight ranges were 100–10,000 for Styragel HT2, 500–30,000 for Styragel HT3, and 5000–600,000 for Styragel HT4, separately. The pore sizes were 50, 100, and 1000 nm for Styragel HT2, HT3, and HT4, respectively. THF was employed
50 as the eluent at a flow rate of 1.0 mL min^{-1} at 35 ℃. All GPC curves were calibrated against a series of monodispersed polystyrene standards. Optical rotation data were collected on a JASCO Model P-1030 digital polarimeter using a water-jacketed 50 mm cell at 25 ℃. UV-Vis absorption spectra were determined
55 on a Varian Cary 1E UV-Vis spectrometer. Circular dichroism (CD) spectra were recorded on a JASCO J-810 with a 10 mm

quartz cell at 25 ℃. The temperature was mediated with a Julabo F25-Me controller. The enantiomer excess was estimated on a high performance liquid chromatography (HPLC) equipped with
60 a JASCO PU-2089 pump, a AS-2055 automatic sampler, a UV-2070 UV-Vis spectrometer, a CD-2095 circular dichroism spectrometer, and a Daicel CHIRALPAK AD-H column. The eluents used were the mixtures of isopropanol and hexane with the compositions of 3/97~20/80 (v/v) dependent of analyte
65 structure.

Monomer synthesis

3-Vinylpicolinonitrile (2). 3-Methylpicolinonitrile (10.0 g, 84.7 mmol) and NBS (15.8 g, 88.9 mmol) were dissolved in 100 mL of CCl$_4$. The mixture was refluxed for 4 hours. During the time,
70 4×50 mg portions of AIBN were added. After cooling the mixture to room temperature and filtrating off the suspended solids, the filtrate was concentrated under vacuum. The residue, which contained the monobromide as well as unreacted 3-methylpicolinonitrile and the relevant dibromide, was mixed with
75 PPh$_3$ (22.3 g, 84.7 mmol) and acetone (150 mL). After refluxing for 4 hours and removal of solvent under vacuum, followed by silica column chromatography with ethyl acetate and methanol as eluents, triphenyl-(2-cyano-pyridin-3-yl)-methylphosphonium bromide was obtained as yellow oil. The phosphonium bromide
80 was then dissolved in 100 mL of CH$_2$Cl$_2$, and 200 mL of aqueous formaldehyde (40%) was then added. The mixture was cooled to 0 ℃. With a rapid stirring, 2 mol/L Na$_2$CO$_3$ aqueous solution (100 mL) was dropped slowly over 0.5 hour. The mixture was stirred for another 2 hours at room temperature. When the
85 reaction was completed, organic layer was collected. Another 2 × 150 mL potions of CH$_2$Cl$_2$ were used to extract the aqueous layer. The organic layers were combined and dried over anhydrous Na$_2$SO$_4$. The solvent was taken away under reduced pressure and the residue was purified by column chromatography on silica gel
90 (CH$_2$Cl$_2$ as eluent) to give 6.1 g of product as white powders. The total yield of the three steps is 55%. ^{1}H-NMR (400 MHz, CDCl$_3$, δ ppm): 5.67-5.70 (d, 1H, =C*H*$_2$), 6.00-6.05 (d, 1H, =C*H*$_2$), 7.05-7.12 (dd, 1H, -C*H*=), 7.49-7.53 (dd, 1H, m-*H* to pyridinyl N)，7.99-8.02 (dd, 1H, p-*H* to pyridinyl N), 8.59-8.60 (dd, 1H, o-*H* to
95 pyridinyl N). ^{13}C-NMR (100 MHz, CDCl$_3$, δ ppm): 116.0, 121.3, 126.8, 130.4, 132.2, 132.9, 137.3, 149.9.

(−)-(*S*)-4-*tert*-Butyl-(3-vinyl-pyridin-2-yl)-oxazoline(1).
Zn(OTf)$_2$ (1.45 g, 4.0 mmol) contained in a dry there-necked flask was heated at 90 ℃ under vacuum over 1 h. Afterwards, the
100 solution of (*S*)-*tert*-leucinol (2.34 g, 20 mmol), 3-vinylpicolinonitrile (2.60 g, 20 mmol) and 2,5-di-tertbutyl-4-methylphenol (22 mg, 0.1 mmol) dissolved in 60 mL of toluene was cannulated into the flask. After refluxing for 24 hours and removal of solvent under vacuum, the residue was dissolved in
105 100 mL of CH$_2$Cl$_2$ and washed with 3×100 mL portions of water. The organic phase was combined and dried over anhydrous Na$_2$SO$_4$. The solvent was taken away under reduced pressure and the residue was purified by column chromatography on silica gel (CH$_2$Cl$_2$/methanol = 100/1, v/v, as eluent) to obtain 2.89 g of
110 product as white crystalline solids. Yield: 65%. ^{1}H-NMR (400 MHz, CDCl$_3$, δ ppm): 1.00 (s, 9H, -C(C*H*$_3$)$_3$), 4.17-4.28 (m, 2H, -OC*H*$_2$-), 4.40-4.45 (m, 1H, -NC*H*-), 5.43-5.46 (d, 1H, =C*H*$_2$), 5.72-5.76 (d, 1H, =C*H*$_2$), 7.35-7.38 (dd, 1H, m-*H* to pyridinyl N), 7.62-7.71 (dd, 1H, -C*H*=), 7.93-7.95 (dd, 1H, p-*H* to pyridinyl N),

8.59-8.60 (dd, 1H, o-*H* to pyridinyl N). ^{13}C-NMR (100 MHz, CDCl$_3$, δ ppm): 26.0, 33.9, 68.4, 77.3, 117.6, 125.0, 133.9, 134.3, 134.5, 144.3, 148.4, 161.8. HRMS *m/z* = 231.14905 (MH$^+$), C$_{14}$H$_{19}$N$_2$O required 231.14919. Specific optical rotation [α]$_{365}^{25}$ = −135.9° (c: 1.0 mg/mL, THF).

(−)-(S)-4-*tert*-Butyl-(3-methyl-pyridin-2-yl)-oxazoline (3). The model compound **3** was prepared with a similar method. Yield: 78%. ^{1}H-NMR (400 MHz, CDCl$_3$, δ ppm): 0.99 (s, 9H, -C(C*H*$_3$)$_3$), 2.64 (s, 3H, -C*H*$_3$), 4.15-4.26 (m, 2H, -OC*H*$_2$-), 4.38-4.43 (m, 1H, -NC*H*-), 7.24-7.28 (dd, 1H, m-*H* to pyridinyl N), 7.58-7.60 (dd, 1H, p-*H* to pyridinyl N), 8.52-8.54 (dd, 1H, o-*H* to pyridinyl N). ^{13}C-NMR (100 MHz, CDCl$_3$, δ ppm): 20.60, 26.0, 33.8, 68.1, 77.2, 124.6, 135.0, 139.3, 145.9, 146.8, 162.2. HRMS *m/z* = 219.14881 (MH$^+$), C$_{13}$H$_{19}$N$_2$O required 219.14919. Specific optical rotation [α]$_{365}^{25}$ = −212.7° (c: 1.0 mg/mL, THF).

Radical polymerization

Into a glass ampule, 0.200 g (0.87 mmol) of **1**, 0.71 mg (0.0043 mmol) of AIBN and 1.0 g of THF (14 mmol) were added. After three freeze-pump-thaw cycles, the tube was sealed under vacuum and put into an oil bath kept at 60 ºC for 24 hours. After polymerization, the reaction mixture was diluted with 10 mL of THF and added dropwise into 150 mL of *n*-hexane with rapid stirring. The precipitate was collected by filtration and dried under vacuum at 40 ºC for 48 hours. Yield: 85%. ^{1}H-NMR (400 MHz, CDCl$_3$, δ ppm): 0.0-1.7 (broad peaks, -C*H*$_2$C*H*- protons in the backbone and –C(C*H*$_3$)$_3$ protons in the oxazoline ring), 2.9-4.5 (broad peaks, -C*H*$_2$C*H*- protons in the oxazoline ring), 6.3-7.8 (broad peaks, m-*H* to pyridinyl N), 8.0-8.8 (broad peaks, o-*H* and p-*H* to pyridinyl N). ^{13}C-NMR (100 MHz, CDCl$_3$, δ ppm): 24.0-27.5 (broad peaks), 32.0-35.0 (broad peaks), 39.0-45.0 (broad peaks), 65.5-69.5 (broad peaks), 74.0-79.5 (broad peaks, overlapped by the triplet peaks of CDCl$_3$), 122.5-126.5 (broad peaks), 133.0-137.7 (broad peaks), 137.7-143.4 (broad peaks), 143.4-148.5 (broad peaks), 160.0-163.2 (broad peaks). M_n= 4.85 ×10^4 Da, *PDI* = 2.27. Specific optical rotation [α]$_{365}^{25}$ = −197.5° (c: 1 mg/mL, THF).

Complexation of P1 with Cu(OTf)$_2$

As a typical procedure, a dry Schlenk tube containing Cu(OTf)$_2$ (109 mg, 0.3 mmol) was heated at 90 ºC under vacuum over 1 h. After that, 4 mL of dry THF was added to dissolve Cu(OTf)$_2$ under N$_2$ atmosphere. Into another dry Schlenk tube, **P1** (46 mg, 0.2 mmol) and 4 mL of THF were added. **P1** solution was cannulated to Cu(OTf)$_2$ solution slowly and smoothly, and the mixture was stirred for 24 h at room temperature. After that, 8 mL of dry THF was added to the tube to dilute the solution, which was then added dropwise into 200 mL of ether. The target complex, **(Cu(II)−P1)**, was obtained by filtration, washed with ether, and dried under vacuum at 40 ºC for 24 h. [PyOx]:[Cu] = 1:1 (determined by gravimetric analysis), chemical formula: C$_{16}$H$_{18}$CuF$_6$N$_2$O$_7$S$_2$. Calcd for C$_{16}$H$_{18}$CuF$_6$N$_2$O$_7$S$_2$: C, 32.46; H, 3.06; N, 4.73. Found: C, 31.77; H, 3.80; N, 4.74. FT-IR (neat, KBr plate, cm^{-1}): 2966, 1630, 1573, 1479, 1454, 1397, 1373, 1261, 1175, 1034, 643, 578, 520 (FT-IR of Cu(OTf)$_2$: 1262, 1178, 1036, 645, 580, 521).

The complexes with various [PyOx] to [Cu] ratio were obtained by changing the feeding amount of Cu(OTf)$_2$.

Complexation of 3 with Cu(OTf)$_2$

The complex of Cu(OTf)$_2$ with **3**, **Cu(II)−3**, was prepared as solution by mixing Cu(OTf)$_2$ and **3** with certain ratio in THF just before use.

General procedure for the catalytic enantioselective D−A reaction by polymeric catalyst

Into a dry Schlenk tube, **Cu(II)−P1** (14.8 mg, containing 0.025 mmol Cu (II)) and THF (2 mL) were added under N$_2$ atmosphere. The mixture was stirred for 2 hours at room temperature until a clear solution was obtained. The substrate, **4b** (67 mg, 0.25 mmol), was added and the mixture was stirred for another 0.5 h. Then, the solution was cooled to 0 ºC and cyclopentadiene (0.15 mL, 1.8 mmol) was added via syringe. The reaction process was monitored by TLC. After full conversion of the substrate, the solution was added into 60 mL ether and the precipitates were separated by filtration. The filtrate was evaporated under vacuum and the residue was purified by column chromatography with ethyl acetate as eluent.

Recycling of catalyst

The collected precipitates of last cycle of D−A reaction were added into a dry Schlenk tube without any other special treatment. After the atmosphere of the tube was replaced by N$_2$, 2 mL of THF was added and stirred over 2 hours. The substrate, **4b** (67 mg, 0.25 mmol), was then added into the tube and stirred for another 0.5 hour. The solution was cooled to 0 ºC and cyclopentadiene (0.15 mL, 1.8 mmol) was added. The reaction process was monitored by TLC. After full conversion of the substrate, the solution was precipitated in ether again, and the catalyst was filtered and collected. The filtrate was evaporated under vacuum and the residue was purified by column chromatography with ethyl acetate as eluent.

**General procedure for the catalytic enantioselective D−A reaction by Cu(II)−3**

Cu(OTf)$_2$ (9.0 mg, 0.025 mmol) contained in a dry Schlenk tube was heated at 90 ºC under vacuum over 1 h. Then, **3** (5.5 mg, 0.025 mmol) dissolved in 2 mL of THF was added in the tube under N$_2$ atmosphere and the mixture was stirred over 2 hours at room temperature. After that, the substrate, **4b** (67 mg, 0.25 mmol), was added and the mixture was stirred for another 0.5 h. The mixture was cooled to 0 ºC and cyclopentadiene (0.15 mL, 1.8 mmol) was added. The reaction process was monitored by TLC. After full conversion of the substrate, the solution was evaporated under vacuum and purified by column chromatography with ethyl acetate as eluent.

Results and Discussion

Synthesis

The synthetic route of target catalyst, **Cu(II)−P1**, is illuminated in Scheme 1. The starting material, 3-methylpicolinonitrile, was first brominated by NBS in CCl$_4$ and then reacted with PPh$_3$ to yield triphenyl-(2-cyano-pyridin-3-yl)-methylphosphonium bromide. The Wittig reaction of this phosphonium salt with formaldehyde in aqueous solution under alkaline condition gave the key intermediate, 2-cyan-3-vinyl-pyridine (**2**). The monomer, (−)-(S)-4-*tert*-butyl-(3-vinyl-pyridin-2-yl)-oxazoline (**1**), was

obtained via the condensation with (*S*)-*tert*-leucinol under the catalysis of Zn(OTf)$_2$ at a yield of 65%.[29, 30] It was converted to the corresponding polymer, **P1**, through radical polymerization in THF induced by AIBN. For comparison, the model compound, (−)-(*S*)-4-*tert*-butyl-(3-mehtyl-pyridin-2-yl)-oxazoline (**3**), was also prepared with a similar method. The structures of key intermediate **2**, monomer **1**, and model compound **3** were throughly characterized by ^{1}H-/^{13}C-NMR and high resolution mass spectrometry. All the data agreed completely with the expected structures.
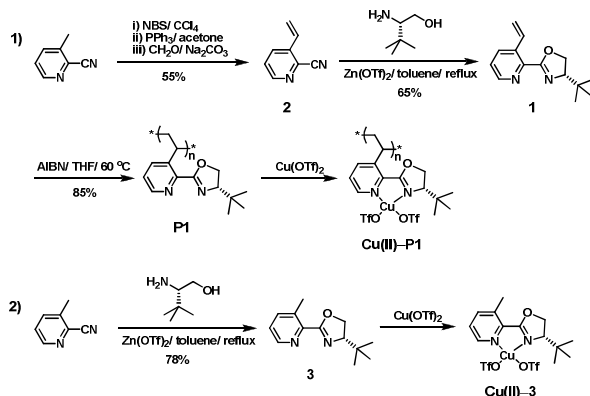
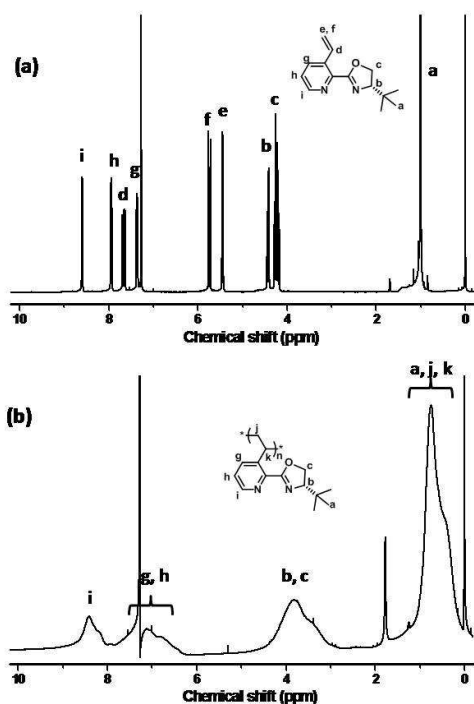**Scheme 1** Syntheses of polymeric catalyst, **Cu(II)–P1**, and its low molecular mass counterpart, **Cu(II)–3**.

Figure 1 ^{1}H-NMR spectra of **1** (a) and **P1** (b) in CDCl$_3$ solution with TMS as an internal standard.

The resultant polymer, **P1**, had a M_n of 4.03×10^4 Da and a molecular weight distribution index (PDI) of 2.27 (M_w/M_n), estimated against polystyrene standards. It was easily dissolved in various solvents, such as THF, methanol, DMF, and CH$_2$Cl$_2$. Figure 1 shows the ^{1}H-NMR spectra of **1** and **P1**. The peaks at 5.43-5.46, 5.72-5.76 and 7.62-7.71 ppm were ascribed to the proton resonances of vinyl group (Figure 1a). They vanished after

polymerization, accompanied with the appearance of broad and weak peaks in the region of 0-1.70 ppm (Figure 1b), implying the formation of polymer backbone. Figure 2 displays the ^{13}C-NMR spectra of **1** and **P1**. The disappearance of vinyl signal at 117.6 ppm and 134.3 ppm (Figure 2a) and the appearance of C–C backbone signal at 39.0-45.0 ppm (Figure 2b) presented the consistent conclusion that the backbone of **P1** formed from vinyl groups of **1**. Due to the limited mobility of protons and carbons, the sharp proton signals and carbon signals of **1** became broad after polymerization. Additionally, carbon signals of C$_H$, which was attaching directly to the polymer backbone, showed diffused peak at 133.0-137.7 ppm, indicating a low tacticity of the polymer.
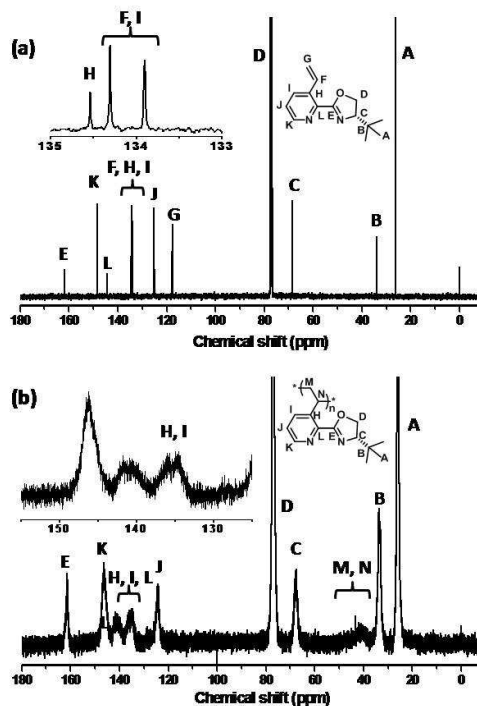

Figure 2 ^{13}C-NMR spectra of **1** (a) and **P1** (b) in CDCl$_3$ solution with TMS as an internal standard.

The complexation of Cu(OTf)$_2$ and **P1** was carried out in THF, in which both reagents were soluble. Whereas, the solubility of the resultant complex **Cu(II)–P1** depended on the feed ratio of Cu(II) and **P1** (Table S1). Since Cu(II) may coordinate with two PyOx groups (Scheme 2a) from different chains and act as a crosslinking point (Scheme 2b), at least a stoichiometric amount of Cu(OTf)$_2$ was required to obtain a soluble complex. In order to guarantee all the PyOx groups are coordinated with Cu(II), the polymer complex used as the catalyst of D−A reaction was prepared by mixing 1.5 molar equivalent of Cu(OTf)$_2$ with **P1**. The polymer complex was obtained by the precipitation of reaction mixture in ether and collected by filtration. Due to the excellent solubility of Cu(OTf)$_2$ in ether, excess Cu(II) salts were washed out with large amount of ether. Based on the gravimetric analysis, the molar ratio of PyOx to Cu(II) ([PyOx]:[Cu]) in the complex obtained was 1:1, which was verified by elementary analysis. The characteristic strong stretching C=N vibration of PyOx group in **3** and **P1** can be seen at 1660 cm^{-1}. It shifts to 1630 cm^{-1} upon Cu(II) coordination (Figure S1). Furthermore, the

FT-IR spectra of **Cu(II)−P1** and **Cu(II)−3** display strong stretching S=O vibrations of triflate ions at 1260 cm^{-1} as Cu(OTf)$_2$, indicating that Cu(OTf)$_2$ coordinates with PyOx in **Cu(II)−P1** and **Cu(II)−3** through Cu−N coordination bond.

The resultant complex was quite stable. Under dry and dark conditions, it showed no change in catalytic activity and enantio-selectivity for over 2 mouths.

Cu(II)−3 was prepared by mixing Cu(OTf)$_2$ and **3** slowly under vigorous stirring. It was used directly as the catalyst. The coordinated solvent could be THF, CH$_2$Cl$_2$ and toluene. The color of the solution was gradually turning from colourless to blue (in THF) or green (in CH$_2$Cl$_2$ or toluene). Due to the good solubility of **Cu(II)−3**, solid complex was not obtained by precipitation as **Cu(II)−P1**.
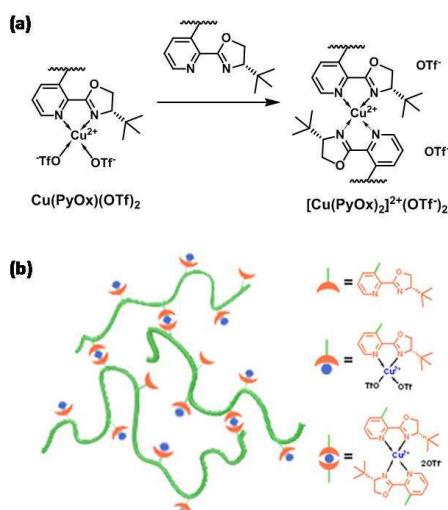
Scheme 2 Excess PyOx groups reacted with [Cu(PyOx)](OTf)$_2$ to form [Cu(PyOx)$_2$](OTf)$_2$ (a). Cross-linking of polymer chains caused by excess PyOx groups (b).

Chiroptical Property

The polymer **P1** showed a specific optical rotation $[\alpha]_{365}^{25}$ of −198°, which was similar to those of the monomer **1** ($[\alpha]_{365}^{25}$ = −136°) and the model compound **3** ($[\alpha]_{365}^{25}$ = −213°). It implied that the optical activity of **P1** might arise solely from the configurational chirality of side-groups and no chiral secondary structure was generated. Figure 3 exhibits the CD and UV-Vis spectra of **1**, **3** and **P1**, recorded in THF solution. **P1** displayed intensive negative Cotton effects centered at 279 nm and two weak positive Cotton effects centered at 250 nm and 225 nm, respectively. Although the electronic transitions of **3** were essentially those of **P1**, its CD pattern was completely different from **P1**. A weak positive band centered at 285 nm and a strong negative one centered at 240 nm were observed. Due to the presence of vinyl group, the UV-Vis absorption spectrum of **1** was distinguished remarkably from those of **3** and **P1**. But it showed a similar CD pattern to **3**. The obvious difference of **P1** to **1** and **3** in CD spectra seemed to suggest the formation of a new chiral structure, such as a helical conformation of polymer backbone with an excess screw sense.

This apparently inconsistent speculation was probably due to the conformation adjustment of side-groups caused by polymerization. The side-groups of **P1** consist of pyridine and oxazoline rings linked by inter-ring C−C bonds. The competition between the conjugative and steric effects results in twisted conformers with various dihedral angles, θ. The population of each conformer depends on their local environments. For **1** and **3**, various conformers interconvert rapidly in solution. However, the interconversion barrier may increase remarkably when the side-groups are closely packed along polymer backbone and favours the formation of a stable rotational isomer, distinct to those of **1** and **3**. This explanation was further proved by the CD spectra of **Cu(II)−3** and **Cu(II)−P1** (Figure 4). When oxazoline and pyridine rings were locked by Cu(II) ion, both complexes should have similar conformations. The small red-shifts in UV-Vis and CD spectra of **3** compared to **P1** might reflect the influence of polymer backbone, i.e. the more crowding environment of **P1** enhanced conjugation.
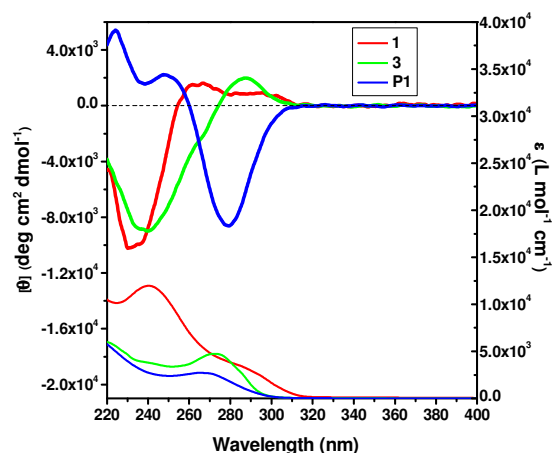

Figure 3 CD and UV-Vis spectra of **1**, **3** and **P1** in THF solution with a concentration of 2 × 10^{-4} mol·L^{-1} recorded at 25 °C.

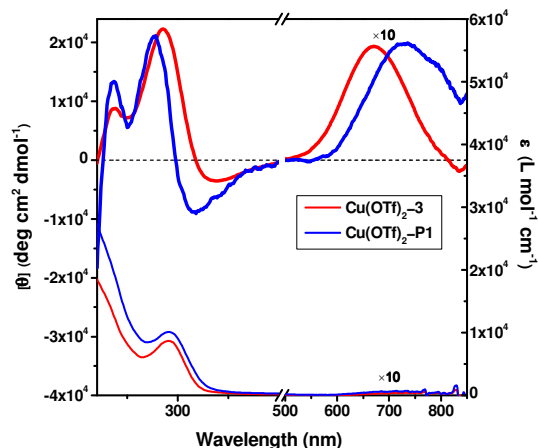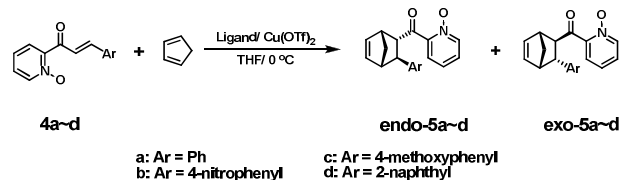**Figure 4** CD and UV-Vis spectra of **Cu(II)−3** and **Cu(II)−P1** in THF solution with a concentration of 9 × 10^{-5} mol·L^{-1} recorded at 25 °C.

D−A Reaction

The D−A reactions of the substrates **4a∼d** with cyclopentadiene were carried out in THF with **Cu(II)−3** and **Cu(II)−P1** as

catalysts, respectively (Scheme 3). The results are summarized in Table 1. For each substrate, both catalysts exhibited excellent diastereo-selectivity over 95/5 (endo/exo). This consistent with the "*endo rule*", which was first proposed by Alder and Stein.[45]

[5] That is, dienophile and diene molecules tend to be arranged face to face rather than head to tail in the transition state of D−A reaction since the former arrangement brings about extra stabilization energy from the dispersive force caused by the polarizability of both reactants, and from secondary binding force

[10] caused by the secondary orbital overlaps of the diene and the carbonyl group of the dienophile.[46-49] The face to face transition state affords the endo adducts.

In addition, the polymeric catalyst displayed a greatly enhanced catalytic efficiency. **Cu(II)−P1** catalyzed the full

[15] conversion of **4b** within 0.2 hour, while **Cu(II)−3** took 1 hour (Entries 3 and 4). The high population of Cu(II)−PyOx groups around polymer backbone, which could bring about higher local concentration of the catalytic sites and coordinated rate of substrate molecules with Cu(II), was supposed to rationalize this

[20] behaviour. Other factors such as the cis or trans form of catalyst might also play an important role. A valid conclusion was not able to obtain right now.

4a~d   **endo-5a~d**   **exo-5a~d**

a: Ar = Ph   c: Ar = 4-methoxyphenyl
b: Ar = 4-nitrophenyl   d: Ar = 2-naphthyl

Scheme 3 D−A reactions of 2-alkenoyl pyridine *N*-oxide **4a~d** and
[25] cyclopentadiene.

Table 1 D−A reaction results of 2-alkenoyl pyridine N-oxide **4a~d** and cyclopentadiene catalyzed by **Cu(II)−P1** or **Cu(II)−3**[a]

Entry	Sub.	Cat.	Temp. (°C)	Time (h)[b]	Yield (%)[c]	endo/exo[d]	ee endo (%)[d]
1	4a	Cu(II)−P1	0	1	97	97:3	42.3
2	4a	Cu(II)−3	0	3	90	97:3	34.3
3	4b	Cu(II)−P1	0	0.2	98	96:4	52.3
4	4b	Cu(II)−3	0	1	92	95:5	21.5
5	4c	Cu(II)−P1	0	1	94	98:2	45.2
6	4c	Cu(II)−3	0	3	93	98:2	39.5
7	4d	Cu(II)−P1	0	0.5	94	97:3	44.8
8	4d	Cu(II)−3	0	2	92	97:3	33.0
9	4a	Cu(OTf)₂	0	5	90	97:3	0.0
10	4a	3	0	72	Null	n. d.	n. d.
11	4a	P1	0	72	Null	n. d.	n. d.
12	4b	Cu(II)−P1	40	<0.1	96	94:6	36.0
13	4b	Cu(II)−3	40	<0.1	95	94:6	20.9
14	4b	Cu(II)−P1	−15	2	96	97:3	56.2
15	4b	Cu(II)−3	−15	12	95	96:4	29.3
16[e]	4b	Cu(II)−P1	0	4	94	97:3	57.5
17[e]	4b	Cu(II)-3	0	12	80	95:5	43.1

[a] All experiments were carried out under nitrogen atmosphere, dienophile (0.25 mmol), Cu(OTf)₂ (0.025 mmol), **3** (0.025 mmol) or
[30] **Cu(II)−P1**(0.025 mmol), cyclopentadiene(1.8 mmol), and THF (2 mL); [b] The time for full conversion monitored by TLC; [c] Isolated product after column separation; [d] Determined by HPLC using a Daicel CHIRALPAK AD-H; [e] H₂O (1.25 mmol) was added before the reaction took place.

Besides the enhanced catalytic activity, **Cu(II)−P1** also
[35] exhibited higher enantio-selectivity than **Cu(II)−3**. Under the catalysis of **Cu(II)−P1**, the major diastereomers **endo-5a~d** were obtained with enantiomeric excess values of 42.3%, 51.3%,

45.2% and 44.8%, respectively. Under the identical condition, **Cu(II)−3** afforded the endo-adduct with ee values of 34.3%,
[40] 21.5%, 39.5% and 33.0%, separately. These results strongly indicated that the attachment of Cu(II)−PyOx pendants to polymer backbone did favour the enantio-selectivity.

Controlled experiments with **4a** as substrate were performed (Entries 9~11, Table 1). Cu(OTf)₂ alone was able to promote the
[45] D−A reaction but displayed no enantio-selectivity. When Cu(OTf)₂ was absent, neither **3** nor **P1** promoted the reaction.

Reaction conditions were optimized to improve enantio-selectivity by using **4b** as the substrate because it yielded the product with the highest ee%. Raising the reaction temperature
[50] from 0 °C to 40 °C had the effect of increasing reaction rate and decreasing diastereo- and enantio-selectivity (Entries 12 and 13, Table 1). On the contrary, when the reaction temperature was reduced to −15 °C, the reaction rate was ten times slower, but the diastereo- and enantio-selectivity were increased (56.2% ee for
[55] **Cu(II)−P1** in Entry 14, and 29.3% ee for **Cu(II)−3** in Entry 15). H₂O can coordinate with Cu(II) much more strongly than triflate. It would be hardly replaced by the substrate molecules in the corresponding complex, which might reduce the reactivity and selectivity of the reactions. To know the effect of water on the
[60] reaction, 5 molar equivalent H₂O was introduced to the reaction system via syringe (Entries 16 and 17). As expected, due to the addition of water, much more time was required to complete the reaction: 4 hours by **Cu(II)−P1** and 12 hours by **Cu(II)−3**. However, the enantio-selectivity increased a little, 57.5% ee
[65] catalyzed by **Cu(II)−P1** and 43.1% ee by **Cu(II)−3**. Although the ee% increased faster in Entry 17, nearly 20% of the substrate **4b** was converted to the by-product. By contrast, no by-product was observed in Entry 16. In other words, there was nearly no negative effect on the **Cu(II)−P1** catalytic reactions when they
[70] were exposed to limited humidity.

Catalytic Mechanism

The proposed catalytic cycle of the D−A reaction is presented in Scheme 4.[50] The dienophile molecule **4** first coordinates with the catalytic side-groups of **Cu(II)−P1** to form the intermediate
[75] **Cu(II)−P1−4**. Owing to the acidity of Cu(II), the LUMO energy of the vinyl group of **4** is reduced, which favors cyclopentadiene addition and yields intermediate **Cu(II)−P1−5** via a transition state. **Cu(II)−P1−5** reacts with **4** to give **Cu(II)−P1−4** again and releases the product **5**. The reaction cycle continues until **4** is
[80] completely converted.
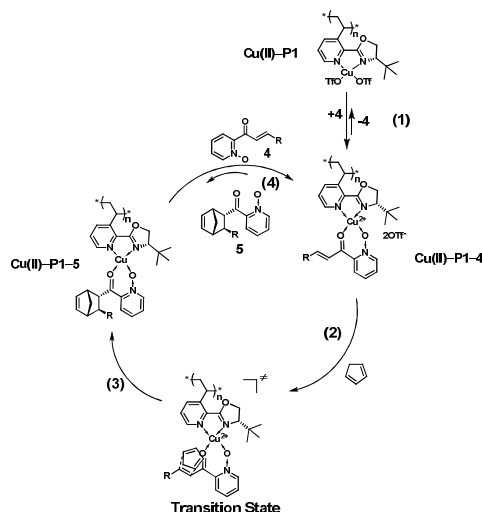
Scheme 4 Proposed Catalytic cycle of substrate **4** reacted with cyclopentadiene by **Cu(II)−P1**.

Based on this mechanism, the enantio-selectivity of the reaction is determined by the direction that cyclopentadiene approach dienophile. Unlike BOX ligand, PyOx group does not have a C_2 symmetric axis. As a result, the intermediate may have two configurations, i.e. cis- and trans-forms (Scheme 5),[51] which are distinguished by the relative position of alkenoyl group and the oxazoline ring because the ligands around the Cu(II) ions take the square-planar configuration.[52] Due to the repulsive force between the phenyl group and the *tert*-butyl group, we suppose that the cis- intermediate configuration is more stable than the trans- one. During D−A reaction, cyclopentadiene prefers to approach the alkenoyl group of the cis-configuration from the opposite face to the *tert*-butyl group, i.e. *α-Si*-face, and gives α-*S* **endo-5** as the major product.
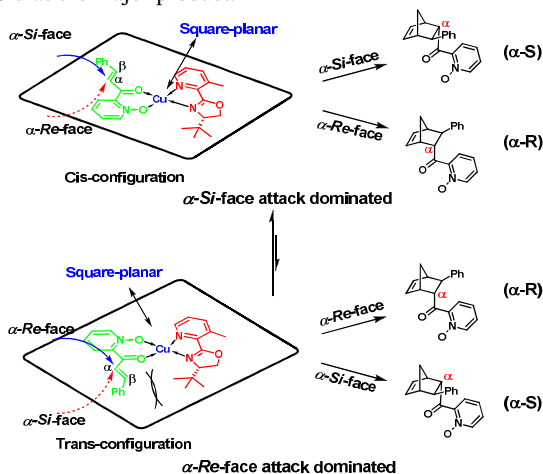
Scheme 5 Proposed reaction mechanism of cyclopentadiene and **Cu(II)−P1−4**.

As demonstrated previously, **Cu(II)−P1** and **Cu(II)−3** displayed similar CD patterns. One may ask what bring about the distinct enantio-selectivity between them in D−A reaction. In order to answer this question, 2 molar equivalent substrate was added into 2 mL of 4.5×10^{-4} mol·L^{-1} THF solutions of **Cu(II)−P1** or **Cu(II)−3**, respectively. After vigorous stirring for over 2 hours at room temperature, the mixture was diluted to 10 mL and characterized by CD spectroscopy. Figure 5 displays the

UV-Vis absorption and CD spectra of **Cu(II)−3**, **Cu(II)−P1**, **Cu(II)−3−4a**, and **Cu(II)−P1−4a**. It was evident that the addition of **4a** caused a remarkable variation in the electronic transition of **Cu(II)−P1**. In the absence of **4a**, the complex showed just an absorption band above 290 nm. When **4a** was added, a new intensive absorption band extending to 500 nm was present, which might originate from the ligand to metal charge transfer (LMCT). Accompanied by the appearance of this absorption, **Cu(II)−P1−4a** displayed a new intensive positive Cotton effect sat 425 nm. In addition, the positive Cotton effects at 230 nm and the negative ones at 305 nm disappeared. It suggested that the coordination of **4a** with **Cu(II)−P1** transferred the chiral message from PyOx group to **4a** and might lead a chiral arrangement of **4a** in space. In a sharp contrast, regardless of the presence of charge transfer absorption in the long wavelength region, the addition of **4a** did not lead to obvious change in the CD spectrum of **Cu(II)−3**. The subtractive CD spectra further demonstrated the distinct role of low and high molecular weight complexes on the chirality of intermediates (Figure 6). The substrates **4c** and **4d** behaved in a similar way (Figures S4~S7). Although both **Cu(II)−P1−4b** and **Cu(II)−3−4b** showed only weak absorptions in the long wavelength region (Figures S2~S3), due to the electron withdrawn nature of nitro group, different CD spectra were also observed. It was considered that the high population of catalytic groups along the polymer backbones provided a confined environment for the substrate molecules to attack and subsequent D−A reaction.
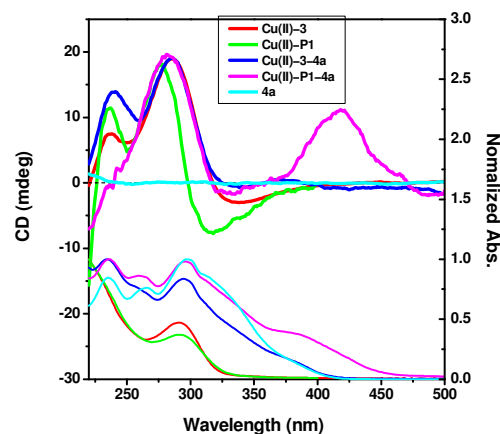

Figure 5 UV-Vis absorption and CD spectra of **Cu(II)−3**, **Cu(II)−P1**, **Cu(II)−3−4a** and **Cu(II)−P1−4a** in THF solution at 25 °C. 2 molar equivalent **4a** was added to **Cu(II)−3** and **Cu(II)−P1** with a concentration of 9×10^{-5} mol·L^{-1}. The UV-Vis spectra were normalized at the highest peaks.
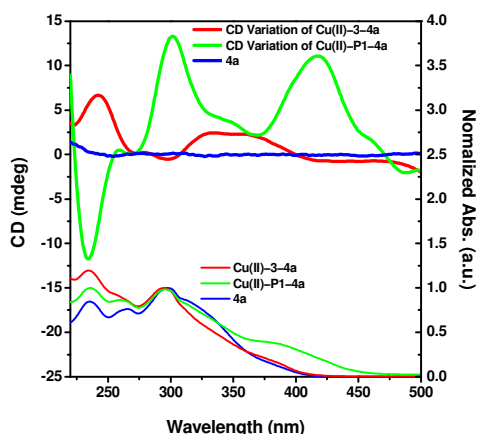
Figure 6 UV-Vis absorption spectra of **Cu(II)–3–4a**, **Cu(II)–P1–4a**, and **4a** in THF solution at 25 °C (lower). CD spectra of **Cu(II)–3–4a** and **Cu(II)–P1–4a** obtained after the subtraction of those of the corresponding complexes (upper). UV-Vis absorption spectra were normalized at 300 nm.

Recycling of Cu(II)−P1

The polymeric catalyst was recycled by precipitating the reaction mixture in ether and filtration after D−A reaction. Without any treatment, it was used to catalyze D−A reaction again. The recycling results are listed in Table 2. The catalytic activity and the enantio-selectivity were diminished slightly as the recycling number increased. After 5 cycles, it took 1 hour for **4b** to be fully converted and the enantio-selectivity decreased from 51.5 ee% to 43.5 ee%. The possible reason of these phenomena was the gradually leaching of the Cu(II) ions from the backbone during recycling.

Table 2 D−A reaction results of 2-alkenoyl pyridine *N*-oxide **4b** and cyclopentadiene catalyzed by **Cu(II)−P1** recycled various times[a]

Cycles	Time (h)	Yield (%)[b]	endo/exo[c]	*ee* endo(%)[c]
1	0.2	96	97:3	51.5
2	0.3	97	96:4	46.1
3	0.3	94	96:4	44.6
4	0.5	93	97:3	44.2
5	0.8	90	97:3	43.3
6	1	90	97:3	43.5

[a] The same reaction conditions as presented in Table 2; **Cu(II)−P1** was recycled by precipitating the reaction solution in ether and filtration; [b] Isolated product after column separation; [c] Determined by HPLC using a Daicel CHIRALPAK AD-H.

Conclusions

In the present work, a novel PyOx containing optically active polymer, **P1**, was obtained. It was converted to the polymeric complex, **Cu(II)−P1**, by the coordination with Cu(OTf)$_2$. Under the catalysis of **Cu(II)−P1**, the homogeneous D−A reactions of 2-alkenyol pyridine *N*-oxide and cyclopentadiene were carried out in tetrahydrofuran. Compared to the low molecular mass model compound, the polymeric catalyst showed a 5 fold faster reaction rate and a 2.5 fold higher enantio-selectivity. It is considered that the high population of Cu(II)−PyOx groups around polymer backbone brings about high local concentration of the catalytic sites and provides constrained environment for D−A reaction, which favours the stereoselectivity. **Cu(II)−P1** was easily recycled by the precipitation method, and only a slight decrease of reactivity and enantio-selectivity was observed after 5 cycles. CD spectrometry was utilized to rationalize the relatively high enantio-selectivity of **Cu(II)−P1** compared to **Cu(II)−3** by virtue of their good solubilities in THF, which may become an efficient method to estimate the enantio-selectivity of some reactions before performing them. Due to the lack of a C$_2$ symmetric axis as in BOX, the interaction of **Cu(II)-P1** with the dienophile **4** yields the intermediates with two configurations, i.e. cis- and trans-forms, which produce various stereoisomers and therefore reduces the stereoselectivity. Increasing the stereoregularity of polymer main chain by employing anionic polymerization to obtain polymer ligand and generating chiral secondary structure by increasing the size of side groups may improve enantio-selectivity. The corresponding work is currently under development in our laboratory.

Acknowledgments

Notes and references

Beijing National Laboratory for Molecular Sciences, Key Laboratory of Polymer Chemistry and Physics of Ministry of Education, College of Chemistry and Molecular Engineering, Peking University, Beijing 100871, China. Email: xhwan@pku.edu.cn; Fax: 86-10-62751708; Tel: 86-10-62754187

† Electronic Supplementary Information (ESI) available: [details of any supplementary information available should be included here]. See DOI: 10.1039/b000000x/

1. E. N. Jacobsen, A. Pfaltz and H. Yamamoto, *Comprehensive Asymmetric Catalysis*, Springer, New York, 1999.
2. K. Mikami and M. Lautens, *New Frontiers in Asymmetric Catalysis*, John Wiley & Sons, Inc., Hoboken, NJ, 2007.
3. I. Ojima, *Catalytic Asymmetric Synthesis*, Wiley, New York, 2009.
4. H. U. Blaser, *Chemical Communications*, 2003, 293-296.
5. D. E. De Vos, I. F. J. Vankelecom and P. A. Jacobs, *Chiral Catalyst Immobilization and Recycling*, Wiley-VCH Verlag GmbH, 2000.
6. S. Itsuno, *Polymeric Chiral Catalyst Design and Chiral Polymer Synthesis*, John Wiley & Sons, Inc., Hoboken, NJ, 2011.
7. K. Soai and M. Watanabe, *Tetrahedron: Asymmetry*, 1991, **2**, 97-100.
8. M. Watanabe and K. Soai, *Journal of the Chemical Society, Perkin Transactions 1*, 1994, 837-842.
9. M. A. Pericàs, D. Castellnou, I. Rodríguez, A. Riera and L. Solà, *Advanced Synthesis & Catalysis*, 2003, **345**, 1305-1313.
10. A. Bastero, D. Font and M. A. Pericàs, *The Journal of Organic Chemistry*, 2007, **72**, 2460-2468.
11. R. P. Megens and G. Roelfes, *Chemistry – A European Journal*, 2011, **17**, 8514-8523.
12. M. Reggelin, M. Schultz and M. Holbach, *Angewandte Chemie International Edition*, 2002, **41**, 1614-1617.
13. C. A. Müller, T. Hoffart, M. Holbach and M. Reggelin, *Macromolecules*, 2005, **38**, 5375-5380.
14. Z. L. Tang, H. Iida, H. Y. Hu and E. Yashima, *ACS Macro Letters*, 2012, **1**, 261-265.
15. W. S. Huang, Q. S. Hu, X. F. Zheng, J. Anderson and L. Pu, *Journal of the American Chemical Society*, 1997, **119**, 4313-4314.
16. T. Yamamoto, T. Yamada, Y. Nagata and M. Suginome, *Journal of the American Chemical Society*, 2010, **132**, 7899-7901.

17. G. Desimoni, G. Faita and K. A. Jørgensen, *Chemical Reviews*, 2011, **111**, PR284-PR437.
18. G. C. Hargaden and P. J. Guiry, *Chemical Reviews*, 2009, **109**, 2505-2550.
19. S. Liao, X. L. Sun and Y. Tang, *Accounts of Chemical Research*, 2014, **47**, 2260-2272.
20. A. Schumacher, M. Bernasconi and A. Pfaltz, *Angew. Chem.*, 2013, 125, 7570-7573.
21. J. Troendlin, J. Rehbein, M. Hiersemann and O. Trapp, *J. Am. Chem. Soc.*, 2011, 133, 16444-16450.
22. J. Rehbein and M. Hiersemann, *J. Org. Chem.*, 2009, 74, 4336-4342.
23. J. Rehbein, S. Leick and M. Hiersemann, *J. Org. Chem.*, 2009, 74, 1531-1540.
24. D. Rechavi and M. Lemaire, *Chemical Reviews*, 2002, **102**, 3467-3494.
25. C. Jönsson, K. Hallman, H. Andersson, G. Stemme, M. Malkoch, E. Malmström, A. Hult and C. Moberg, *Bioorganic & Medicinal Chemistry Letters*, 2002, **12**, 1857-1861.
26. J. M. Fraile, J. I. García and J. A. Mayoral, *Coordination Chemistry Reviews*, 2008, **252**, 624-646.
27. E. Framery, B. Andrioletti and M. Lemaire, *Tetrahedron: Asymmetry*, 2010, **21**, 1110-1124.
28. R. Breslow and M. Schmir, *Journal of the American Chemical Society*, 1971, **93**, 4960-4961.
29. C. Bolm, K. Weickhardt, M. Zehnder and T. Ranff, *Chem. Ber.*, 1991, **124**, 1173-1178.
30. A. Cornejo, J. M. Fraile, J. I. García, M. J. Gil, V. Martínez-Merino, J. A. Mayoral, E. Pires and I. Villalba, *Synlett*, 2005, 2321-2324.
31. U. Bremberg, F. Rahm and C. Moberg, *Tetrahedron: Asymmetry*, 1998, **9**, 3437-3443.
32. G. Chelucci, S. Medici and A. Saba, *Tetrahedron: Asymmetry*, 1999, **10**, 543-550.
33. Y. Zhang and M. S. Sigman, *Journal of the American Chemical Society*, 2007, **129**, 3076-3077.
34. E. W. Werner, T. S. Mei, A. J. Burckle and M. S. Sigman, *Science*, 2012, **338**, 1455-1458.
35. Y. Dang, S. Qu, Z. X. Wang and X. Wang, *Journal of the American Chemical Society*, 2013, **136**, 986-998.
36. J. C. Holder, L. Zou, A. N. Marziale, P. Liu, Y. Lan, M. Gatti, K. Kikushima, K. N. Houk and B. M. Stoltz, *Journal of the American Chemical Society*, 2013, **135**, 14996-15007.
37. R. I. McDonald, P. B. White, A. B. Weinstein, C. P. Tam and S. S. Stahl, *Organic Letters*, 2011, **13**, 2830-2833.
38. A. B. Weinstein and S. S. Stahl, *Angewandte Chemie International Edition*, 2012, **51**, 11505-11509.
39. S. Reymond and J. Cossy, *Chemical Reviews*, 2008, **108**, 5359-5406.
40. H. Brunner and P. Brandl, *Zeitschrift fuer Naturforschung, B: Chemical Sciences*, 1992, **47**, 609-613.
41. M. Malkoch, K. Hallman, S. Lutsenko, A. Hult, E. Malmström and C. Moberg, *The Journal of Organic Chemistry*, 2002, **67**, 8197-8202.
42. C. Aranda, A. Cornejo, J. M. Fraile, E. Garcia-Verdugo, M. J. Gil, S. V. Luis, J. A. Mayoral, V. Martinez-Merino and Z. Ochoa, *Green Chemistry*, 2011, **13**, 983-990.
43. V. Chiroli, M. Benaglia, A. Puglisi, R. Porta, R. P. Jumde and A. Mandoli, *Green Chem.*, 2014, 16, 2798-2806
44. S. Barroso, G. Blay and J. R. Pedro, *Organic Letters*, 2007, **9**, 1983-1986.
45. K. Alder and G. Stein, *Angewandte Chemie*, 1937, **50**, 510-519.
46. R. B. Woodward and T. J. Katz, *Tetrahedron*, 1959, **5**, 70-89.
47. K. Seguchi, A. Sera and K. Maruyama, *Tetrahedron Letters*, 1973, **14**, 1585-1588.
48. B. S. El'yanov, S. K. Shakhova, B. D. Polkovnikov and L. F. Rar, *Journal of the Chemical Society, Perkin Transactions 2*, 1985, 11-16.
49. A. V. George and N. S. Isaacs, *Journal of the Chemical Society, Perkin Transactions 2*, 1985, 1845-1847.
50. S. Otto, F. Bertoncin and J. B. F. N. Engberts, *Journal of the American Chemical Society*, 1996, **118**, 7702-7707.
51. S. Otto and J. B. F. N. Engberts, *Journal of the American Chemical Society*, 1999, **121**, 6798-6806.
52. D. A. Evans, S. J. Miller, T. Lectka and P. von Matt, *Journal of the American Chemical Society*, 1999, **121**, 7559-7573.